FERMILAB-PUB-10-456-AE-CD-E

Results from a Low-Energy Analysis of the CDMS II Germanium Data

Z. Ahmed,[1] D.S. Akerib,[2] S. Arrenberg,[19] C.N. Bailey,[2] D. Balakishiyeva,[17] L. Baudis,[19] D.A. Bauer,[3] P.L. Brink,[7] T. Bruch,[19] R. Bunker,[15] B. Cabrera,[11] D.O. Caldwell,[15] J. Cooley,[10] P. Cushman,[18] M. Daal,[14] F. DeJongh,[3] M.R. Dragowsky,[2] L. Duong,[18] S. Fallows,[18] E. Figueroa-Feliciano,[5] J. Filippini,[1] M. Fritts,[18] S.R. Golwala,[1] J. Hall,[3] R. Hennings-Yeomans,[2] S.A. Hertel,[5] D. Holmgren,[3] L. Hsu,[3] M.E. Huber,[16] O. Kamaev,[18] M. Kiveni,[12] M. Kos,[12] S.W. Leman,[5] R. Mahapatra,[13] V. Mandic,[18] K.A. McCarthy,[5] N. Mirabolfathi,[14] D. Moore,[1,*] H. Nelson,[15] R.W. Ogburn,[11] A. Phipps,[14] M. Pyle,[11] X. Qiu,[18] E. Ramberg,[3] W. Rau,[6] A. Reisetter,[18,8] T. Saab,[17] B. Sadoulet,[4,14] J. Sander,[15] R.W. Schnee,[12] D.N. Seitz,[14] B. Serfass,[14] K.M. Sundqvist,[14] M. Tarka,[19] P. Wikus,[5] S. Yellin,[11,15] J. Yoo,[3] B.A. Young,[9] and J. Zhang[18]

(CDMS Collaboration)

[1] *Division of Physics, Mathematics & Astronomy, California Institute of Technology, Pasadena, CA 91125, USA*
[2] *Department of Physics, Case Western Reserve University, Cleveland, OH 44106, USA*
[3] *Fermi National Accelerator Laboratory, Batavia, IL 60510, USA*
[4] *Lawrence Berkeley National Laboratory, Berkeley, CA 94720, USA*
[5] *Department of Physics, Massachusetts Institute of Technology, Cambridge, MA 02139, USA*
[6] *Department of Physics, Queen's University, Kingston, ON, Canada, K7L 3N6*
[7] *SLAC National Accelerator Laboratory/KIPAC, Menlo Park, CA 94025, USA*
[8] *Department of Physics, St. Olaf College, Northfield, MN 55057 USA*
[9] *Department of Physics, Santa Clara University, Santa Clara, CA 95053, USA*
[10] *Department of Physics, Southern Methodist University, Dallas, TX 75275, USA*
[11] *Department of Physics, Stanford University, Stanford, CA 94305, USA*
[12] *Department of Physics, Syracuse University, Syracuse, NY 13244, USA*
[13] *Department of Physics, Texas A & M University, College Station, TX 77843, USA*
[14] *Department of Physics, University of California, Berkeley, CA 94720, USA*
[15] *Department of Physics, University of California, Santa Barbara, CA 93106, USA*
[16] *Departments of Phys. & Elec. Engr., University of Colorado Denver, Denver, CO 80217, USA*
[17] *Department of Physics, University of Florida, Gainesville, FL 32611, USA*
[18] *School of Physics & Astronomy, University of Minnesota, Minneapolis, MN 55455, USA*
[19] *Physics Institute, University of Zürich, Winterthurerstr. 190, CH-8057, Switzerland*

We report results from a reanalysis of data from the Cryogenic Dark Matter Search (CDMS II) experiment at the Soudan Underground Laboratory. Data taken between October 2006 and September 2008 using eight germanium detectors are reanalyzed with a lowered, 2 keV recoil-energy threshold, to give increased sensitivity to interactions from Weakly Interacting Massive Particles (WIMPs) with masses below $\sim$10 GeV/c^2. This analysis provides stronger constraints than previous CDMS II results for WIMP masses below 9 GeV/c^2 and excludes parameter space associated with possible low-mass WIMP signals from the DAMA/LIBRA and CoGeNT experiments.

PACS numbers: 14.80.Ly, 95.35.+d, 95.30.Cq, 95.30.-k, 85.25.Oj, 29.40.Wk

A convergence of astrophysical observations indicates that $\sim$80% of the matter in the universe is in the form of non-baryonic, non-luminous dark matter [1]. Weakly Interacting Massive Particles (WIMPs) [2], with masses from a few GeV/c^2 to a few TeV/c^2, form a well-motivated class of candidates for this dark matter [1, 3]. If WIMPs account for the dark matter, they may be detectable through their elastic scattering with nuclei in terrestrial detectors [4].

Although many models of physics beyond the Standard Model provide WIMP candidates, supersymmetric (SUSY) models where the lightest superpartner is a cosmologically stable WIMP are among the most popular [1, 3]. In the simplest SUSY models, WIMPs with masses $\lesssim$40 GeV/c^2 are generally disfavored by accelerator constraints (e.g., [5]). Interest in lower-mass WIMPs has been renewed by recent results from the DAMA/LIBRA [6] and CoGeNT [7] experiments, which have been interpreted in terms of elastic scatters from a WIMP with mass $\sim$10 GeV/c^2 and cross-section $\sim 10^{-40}$ cm^2 [8, 9]. Although it is difficult to accommodate a WIMP with these properties in the Minimal Supersymmetric Standard Model (MSSM) [10], relatively simple extensions to the MSSM can avoid existing constraints [11]. More complicated models which allow for $\sim$10 GeV/c^2 WIMPs have also been proposed (e.g., [12]).

The CDMS II experiment attempts to identify nuclear recoils from WIMPs in an array of particle detectors by measuring both the ionization and non-equilibrium phonons created by each particle interaction. Backgrounds can be rejected on an event-by-event basis since they primarily scatter from electrons in the detector, de-

positing significantly more ionization than a nuclear recoil of the same energy. Previous analyses of CDMS II data [13] imposed a recoil-energy threshold of 10 keV to maintain sufficient rejection of electron recoils that only ∼0.5 background events would be expected in the signal region. At lower energies, the discrimination between nuclear and electron recoils degrades, leading to higher expected backgrounds. Since WIMPs with masses <10 GeV/c^2 primarily produce <10 keV recoils, this analysis lowers the recoil-energy threshold to 2 keV, comparable to the hardware trigger threshold. This lower energy threshold increases sensitivity to low-mass WIMPs at the cost of significant acceptance of backgrounds.

The data analyzed here were collected using all 30 Z-sensitive Ionization and Phonon (ZIP) detectors installed at the Soudan Underground Laboratory [13, 14]. The detector array consisted of 19 Ge (∼230 g each) and 11 Si (∼105 g each) detectors, each of which is a disk ∼10 mm thick and 76 mm in diameter. Each detector was instrumented with four phonon sensors on one face and two concentric charge electrodes on the opposite face. A small electric field (3–4 V/cm) was applied across the detectors to extract charge carriers created by particle interactions. The detectors were arranged in five stacks, or "towers," and are identified by their tower number (T1–T5) and by their ordering within the tower (Z1–Z6). The entire array was cooled to $\lesssim$50 mK and surrounded by passive lead and polyethylene shielding. An outer plastic scintillator veto was used to identify showers containing cosmogenic muons which were not shielded by the rock overburden above the Soudan laboratory (2090 meters water equivalent).

The data were taken during six data runs from October 2006 to September 2008 [13]. Only the eight Ge detectors with the lowest trigger thresholds were used to identify WIMP candidate events since they have the best expected sensitivity to WIMPs with masses from 5–10 GeV/c^2. All 30 detectors were used to veto events which deposited energy in multiple detectors.

Stability throughout the data-taking periods was monitored on a detector-by-detector basis using Kolmogorov-Smirnov tests, and periods of abnormal detector performance were removed. The ratio of ionization to recoil energy ("ionization yield") for electron recoils was also monitored in order to exclude data periods showing evidence of reduced ionization collection. Data taken within 20 days following exposure of the detectors to a neutron calibration source were removed to reduce low-energy electron-recoil backgrounds due to activation of the detectors. The data were randomly divided into two subsets before defining selection criteria at low energy. One subset, consisting of one quarter of the data (the "open" data), was reserved to study backgrounds at low energy and was not used to calculate exclusion limits. The remaining subset totaled 241 kg days raw exposure, after removing the bad data periods described above.

The detector response to electron and nuclear recoils was calibrated by regular exposures of the detectors to γ-ray (^{133}Ba) and neutron (^{252}Cf) sources. The ionization energy scale was calibrated using the 356 keV line from the ^{133}Ba source. The phonon energy was then calibrated by normalizing the phonon-based recoil energy for electron recoils to their mean ionization energy. In contrast to previous analyses, a position-dependent calibration was not applied since position-dependent variations in the reconstructed phonon energies are less significant than noise fluctuations at low energies. The energy scale for electron recoils was verified using activation lines at 1.3 keV and 10.4 keV produced from exposure of the Ge detectors to the ^{252}Cf source. For nuclear recoils, the recoil energy was reconstructed from the measured phonon energy alone by subtracting the Neganov-Luke phonon contribution [15] corresponding to the mean ionization measured for nuclear recoils of the same phonon energy from the ^{252}Cf source. The ionization yield for nuclear recoils was measured down to ∼4 keV, below which a power-law extrapolation was used.

Candidate events were required to pass basic reconstruction quality cuts similar to the criteria used in previous analyses of these data [13]. Due to the negligible probability of a WIMP interacting more than once in the apparatus, candidates were required to have energies consistent with noise in all but one detector and have no coincident activity in the plastic scintillator veto. They were further required to have ionization signals consistent with noise in the outer charge electrode. The ionization energy was required to be within $(+1.25, -0.5)\sigma$ of the mean ionization energy for nuclear recoils measured from calibration data, which defines the "nuclear-recoil band." This asymmetric band was chosen based on calibration data and the observed low-energy backgrounds in the open data, in order to maximize sensitivity to nuclear recoils while limiting leakage from electron recoils and zero-charge events. The recoil-energy range considered for this analysis was 2–100 keV.

The hardware trigger efficiency was determined using events for which at least one other detector triggered, which provide an unbiased selection of events near threshold. The data are well described by an error function, with the mean trigger threshold varying from 1.5–2.5 keV for the eight Ge detectors. Based on the selection criteria above, the signal acceptance was measured using nuclear recoils from the ^{252}Cf calibration data. The livetime-weighted average of the individual detector selection efficiencies is shown in the inset of Fig. 1, with the largest loss of efficiency coming from the requirement on ionization energy.

The energy spectrum for the candidate events passing all selection cuts is shown in Fig. 1. Although the shape of the observed spectrum is consistent with a WIMP signal, the majority of the candidates appear to arise from unrejected electron recoils. Figure 2 shows the distribu-

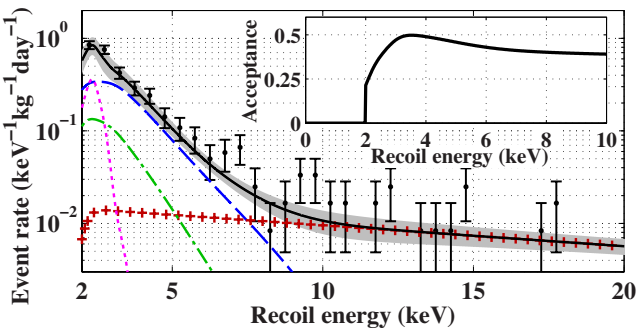

FIG. 1. (color online). Comparison of the energy spectra for the candidate events and background estimates, co-added over the 8 detectors used in this analysis. The observed event rate (error bars) agrees well with the electron-recoil background estimate (solid), which is a sum of the contributions from zero-charge events (dashed), surface events (+), bulk events (dash-dotted), and the 1.3 keV line (dotted). The gray band denotes the 1σ statistical errors on the background estimate. The selection efficiencies have been applied to the background estimates for direct comparison with the observed rate, which does not include a correction for the nuclear-recoil acceptance. The inset shows the measured nuclear-recoil acceptance efficiency, averaged over all detectors.

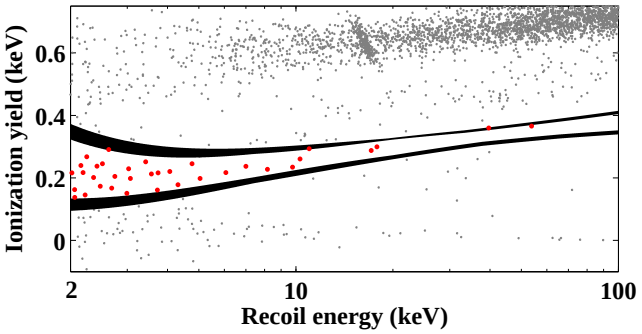

FIG. 2. (color online). Events in the ionization-yield versus recoil-energy plane for T1Z5. Events lying within the $(+1.25, -0.5)\sigma$ nuclear-recoil band (solid) are WIMP candidates (large dots). Events lying outside these bands (small dots) pass all selection criteria except the ionization-energy requirement. The widths of the band edges denote variations between data runs. The recoil-energy scale assumes the ionization signal is consistent with a nuclear recoil, causing electron recoils to be shifted to higher recoil energies and lower yields.

tion of candidates in the ionization-yield versus recoil-energy plane for T1Z5. A band of events with ionization energies consistent with noise is seen below the nuclear-recoil band. Most or all of these "zero-charge" events arise from electron recoils near the edge of the detector, where the charge carriers can be completely collected on the cylindrical wall rather than on the readout electrodes. At recoil energies $\gtrsim$10 keV, these events can be rejected using a phonon-based fiducial-volume cut; however, at lower energies, reconstruction of the event radius using phonon information is unreliable. To maintain acceptance of low-energy nuclear recoils, some zero-charge events are not rejected at energies $\lesssim$5 keV where the ionization signal for nuclear recoils becomes comparable to noise. By extrapolating the exponential spectrum observed for zero-charge events above 5 keV, we estimate that they contribute 40–60% of the candidate events.

A second source of misidentified electron recoils comes from events interacting near the detector surfaces, where ionization collection may be incomplete. These events are primarily concentrated in a band above the nuclear-recoil band but below the bulk electron recoils, with an increased fraction leaking into the signal region at low energies. For recoil energies $\gtrsim$10 keV, nearly all such surface events can be rejected [13] because they have faster-rising phonon pulses than nuclear recoils in the bulk of the detector. This analysis does not use phonon timing to reject these events since the signal-to-noise is too low for this method to be effective for recoil energies $\lesssim$5 keV. Extrapolating the exponential spectrum of surface events identified above 10 keV implies that 10–20% of the candidates are surface electron recoils.

At recoil energies $\lesssim$5 keV, the primary ionization-based discrimination breaks down as the ionization signal becomes comparable to noise even for electron recoils with fully collected charge. Extrapolating the roughly constant electron-recoil spectrum observed above 5 keV indicates that 10–15% of the observed candidates arise from leakage of this background into the signal region. As shown in Fig. 2, T1Z5 has less leakage from this background than the average detector since it has the best ionization resolution. Just above threshold, there is an additional contribution to the constant electron-recoil spectrum from the 1.3 keV line, which leaks above the 2 keV analysis threshold since our recoil-energy estimate assumes the ionization signal is consistent with a nuclear recoil. The measured intensity of this line at ionization yields above the signal region indicates that the 1.3 keV line accounts for 5–15% of the observed candidates.

Monte Carlo simulations indicate that neutrons, whose nuclear recoils are indistinguishable from WIMPs, produce a negligible $\lesssim$0.2 event background.

As shown in Fig. 1, the observed candidate spectrum can be accounted for with known backgrounds, and there is no evidence for a signal. However, since the background model involves sufficient extrapolation that systematic errors are difficult to quantify, we do not subtract this background but instead set upper limits on the allowed WIMP-nucleon scattering cross section by conservatively assuming all observed events could be from WIMPs. Limits are calculated using the high statistics version of Yellin's optimum interval method [21]. Data from multiple detectors are concatenated as described in [16] due to the presence of significant backgrounds, which are expected to vary by detector. The candidate

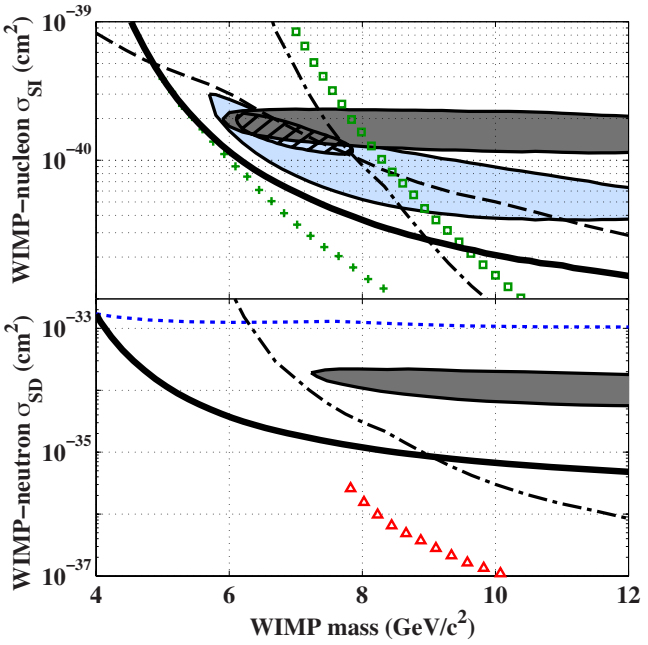

FIG. 3. (color online). Top: comparison of the spin-independent (SI) exclusion limits from these data (solid) to previous results in the same mass range (all at 90% C.L.). Limits from a low-threshold analysis of the CDMS shallow-site data [16] (dashed), CDMS II Ge results with a 10 keV threshold [13] (dash-dotted), recalculated for lower WIMP masses, and XENON100 with constant (+) or decreasing (□) scintillation-efficiency extrapolations at low energy [17] are also shown. The filled regions indicate possible signal regions from DAMA/LIBRA [6, 8] (dark), CoGeNT (light) [7, 8], and a combined fit to the DAMA/LIBRA and CoGeNT data [8] (hatched). Bottom: comparison of the WIMP-neutron spin-dependent (SD) exclusion limits from these data (solid), CDMS II Ge results with a 10 keV threshold (dash-dotted), XENON10 [18] (△), and CRESST [19] (dotted). The filled region denotes the 99.7% C.L. DAMA/LIBRA allowed region for neutron-only scattering [20]. An escape velocity of 544 km/s was used for the CDMS and XENON100 exclusion limits, whereas the other results assume an escape velocity from 600–650 km/s.

event energies and selection efficiencies for each detector are given in [22]. For this analysis, energy intervals from T1Z5 provide the strongest constraints in the 5–10 GeV/c^2 mass range. The standard halo model described in [23] is used, with specific parameters given in [16, 22].

The limits do not depend strongly on the extrapolation of the ionization yield used at low energies since the Neganov-Luke phonon contribution is small for recoil energies below 4 keV. Conservatively assuming 50% lower ionization yield near threshold would lead to only ∼5% weaker limits in the 5–10 GeV/c^2 mass range.

Figure 3 (upper panel) compares the 90% upper confidence limit on the spin-independent WIMP-nucleon scattering cross section from this analysis to previous results in the same mass range. This analysis provides stronger limits than previous CDMS II Ge results for WIMP masses below ∼9 GeV/c^2, and excludes parameter space previously excluded only by the XENON100 experiment assuming a constant extrapolation of the liquid xenon scintillation response for nuclear recoils below 5 keV [17]. This parameter space is not excluded by XENON100 when more conservative assumptions for the scintillation response are used [8, 17, 24].

Spin-dependent limits on the WIMP-neutron cross section are shown in Fig. 3 (lower panel), using the form factor from [25]. XENON10 constraints, calculated assuming a constant extrapolation of the scintillation response at low energy [18, 24], are stronger than these results for WIMP masses above ∼7 GeV/c^2.

These results exclude interpretations of the DAMA/LIBRA annual modulation signal in terms of spin-independent elastic scattering of low-mass WIMPs (e.g., [8, 26]). We ignore the effect of ion channeling on the DAMA/LIBRA allowed regions since recent analyses indicate channeling should be negligible [26]. These results are also incompatible with a low-mass WIMP explanation for the low-energy events seen in CoGeNT [7, 8].

The CDMS collaboration gratefully acknowledges the contributions of numerous engineers and technicians; we would like to especially thank Jim Beaty, Bruce Hines, Larry Novak, Richard Schmitt and Astrid Tomada. In addition, we gratefully acknowledge assistance from the staff of the Soudan Underground Laboratory and the Minnesota Department of Natural Resources. This work is supported in part by the National Science Foundation (Grant Nos. AST-9978911, PHY-0542066, PHY-0503729, PHY-0503629, PHY-0503641, PHY-0504224, PHY-0705052, PHY-0801708, PHY-0801712, PHY-0802575, PHY-0847342, and PHY-0855525), by the Department of Energy (Contracts DE-AC03-76SF00098, DE-FG02-91ER40688, DE-FG02-92ER40701, DE-FG03-90ER40569, and DE-FG03-91ER40618), by the Swiss National Foundation (SNF Grant No. 20-118119), and by NSERC Canada (Grant SAPIN 341314-07).

* Corresponding author: davidm@caltech.edu

[1] G. Bertone, D. Hooper, and J. Silk, Phys. Rep., **405**, 279 (2005).
[2] G. Steigman and M. S. Turner, Nucl. Phys. B, **253**, 375 (1985).
[3] G. Jungman, M. Kamionkowski, and K. Griest, Phys. Rep., **267**, 195 (1996).
[4] M. W. Goodman and E. Witten, Phys. Rev. D, **31**, 3059 (1985); R. J. Gaitskell, Ann. Rev. Nucl. Part. Sci., **54**, 315 (2004).
[5] E. A. Baltz and P. Gondolo, JHEP, **10**, 052 (2004); A. Heister *et al.*, Phys. Lett. B, **583**, 247 (2004).
[6] R. Bernabei *et al.* (DAMA/LIBRA), Eur. Phys. J. C, **56**,

333 (2008); R. Bernabei *et al.*, *ibid.*, **67**, 39 (2010).
[7] C. E. Aalseth *et al.* (CoGeNT), arXiv:1002.4703v2 (2010).
[8] D. Hooper *et al.*, arXiv:1007.1005v3 (2010).
[9] A. L. Fitzpatrick, D. Hooper, and K. M. Zurek, Phys. Rev. D, **81**, 115005 (2010); S. Chang *et al.*, JCAP, **08**, 18 (2010); S. Andreas *et al.*, Phys. Rev. D, **82**, 043522 (2010).
[10] E. Kuflik, A. Pierce, and K. M. Zurek, Phys. Rev. D, **81**, 111701 (2010); D. Feldman, Z. Liu, and P. Nath, *ibid.*, **81**, 117701 (2010); D. Hooper and T. Plehn, Phys. Lett. B, **562**, 18 (2003).
[11] A. V. Belikov *et al.*, arXiv:1009.0549v1 (2010); A. Bottino *et al.*, Phys. Rev. D, **69**, 037302 (2004); G. Bélanger *et al.*, JHEP, **03**, 12 (2004).
[12] J. L. Feng, J. Kumar, and L. E. Strigari, Phys. Lett. B, **670**, 37 (2008); S. Andreas, T. Hambye, and M. H. G. Tytgat, JCAP, **10**, 34 (2008); K. M. Zurek, Phys. Rev. D, **79**, 115002 (2009).
[13] Z. Ahmed *et al.* (CDMS), Phys. Rev. Lett., **102**, 011301 (2009); Science, **327**, 1619 (2010).
[14] D. S. Akerib *et al.* (CDMS), Phys. Rev. D, **72**, 052009 (2005).
[15] B. Neganov and V. Trofimov, Otkryt. Izobret., **146**, 215 (1985); P. N. Luke, J. Appl. Phys., **64**, 6858 (1988).
[16] D. Akerib *et al.* (CDMS), arXiv:1010.4290v1 (2010).
[17] E. Aprile *et al.* (XENON100), Phys. Rev. Lett., **105**, 131302 (2010).
[18] J. Angle *et al.* (XENON10), Phys. Rev. Lett., **101**, 091301 (2008).
[19] G. Angloher *et al.* (CRESST), Astropart. Phys., **18**, 43 (2002); C. Savage, P. Gondolo, and K. Freese, Phys. Rev. D, **70**, 123513 (2004).
[20] C. Savage *et al.*, JCAP, **04**, 10 (2009).
[21] S. Yellin, Phys. Rev. D, **66**, 032005 (2002); arXiv:0709.2701v1 (2007).
[22] See EPAPS Document No. XXX for a complete list of the candidate event energies and detector selection efficiencies needed to reproduce these limits. For more information on EPAPS, see http://www.aip.org/pubservs/epaps.html.
[23] J. D. Lewin and P. F. Smith, Astropart. Phys., **6**, 87 (1996).
[24] J. I. Collar and D. N. McKinsey, arXiv:1005.0838v3 (2010).
[25] V. I. Dimitrov, J. Engel, and S. Pittel, Phys. Rev. D, **51**, R291 (1995).
[26] C. Savage *et al.*, arXiv:1006.0972v2 (2010); N. Bozorgnia, G. B. Gelmini, and P. Gondolo, arXiv:1006.3110v1 (2010).